Technical University of Denmark

Implementation and validation of synthetic inertia support employing series produced electric vehicles

Rezkalla, Michel M.N.; Martinenas, Sergejus; Zecchino, Antonio; Marinelli, Mattia; Rikos, Evangelos

Published in:
Cired - Open Access Proceedings Journal

Link to article, DOI:
10.1049/oap-cired.2017.0686

Publication date:
2017

Document Version
Publisher's PDF, also known as Version of record

Citation (APA):
Rezkalla, M. M. N., Martinenas, S., Zecchino, A., Marinelli, M., & Rikos, E. (2017). Implementation and validation of synthetic inertia support employing series produced electric vehicles. Cired - Open Access Proceedings Journal, 2017(1), 1197 – 1201. DOI: 10.1049/oap-cired.2017.0686

24th International Conference & Exhibition on Electricity Distribution (CIRED)

12-15 June 2017

Session 3: Operation, control and protection

Implementation and validation of synthetic inertia support employing series produced electric vehicles

ISSN 2515-0855
doi: 10.1049/oap-cired.2017.0686
www.ietdl.org

Michel Rezkalla[1] ✉, Sergejus Martinenas[1], Antonio Zecchino[1], Mattia Marinelli[1], Evangelos Rikos[2]

[1]*Technical University of Denmark, Kongens Lyngby, Denmark*
[2]*Center for Renewable Energy Sources, Pikermi, Greece*
✉ *E-mail: mirez@elektro.dtu.dk*

Abstract: The high integration of renewable energy resources (inverter connected) replacing conventional generation reduces the available rotational inertia in the power system. This introduces the need for faster regulation services, including synthetic inertia services. These services could potentially be provided by electric vehicles (EVs) due to their fast response capability. This work evaluates and experimentally shows the capability and limits of EVs in providing synthetic inertia services. Three series-produced EVs are used during the experiment. The results show the performance of the EVs in providing synthetic inertia. It shows also that, on the contrary of synchronous inertia, synthetic inertia might lead to unstable frequency behaviour.

1 Introduction

The displacement of conventional generation by converter connected resources reduces the available rotational inertia in the power system, which leads to faster frequency dynamics and consequently a less stable frequency behaviour [1]. One of the main concerns of transmission system operators (TSOs) is the fast rate of change of frequency (RoCoF) which might lead to a cascade tripping of conventional and distributed generators connected by means of RoCoF relays [2, 3].

Traditionally, inertial response has not been considered as an ancillary service, but rather as a natural characteristic of the power system. Owing to the high integration of converter connected resources, several TSOs began to recognise the value of synthetic inertia response [4, 5].

Simultaneously, the growing number of electric vehicles (EVs), on the one hand, is seen as an additional load on the grid from system operators' perspective. On the other hand, EVs are also one of the candidates for providing grid regulation services (i.e. frequency and voltage control) due to their fast response capability [6, 7]. In principle, they are able to provide fast regulating power in both directions in the case of vehicle-to-grid (V2G), or just to modulate the charging power [8]. Nevertheless, EV's technical characteristics introduce different challenges such as limited individual power and energy ratings, single-phase connection that imply potential source of unbalances and fast, but variable response time.

The total response time of the EV can be divided into different parts:

- Measurement time, which is the time necessary to the measurement device to measure the controller input signal.
- Communication time, which is the time required to send the control signal from the metering location to the location where the EVs are connected to the grid. The two locations can be identical, but it is possible actually to remotely control the EVs as explained in [7].
- EVs' response time, which is the time necessary for ramping up (or down) the power to meet the requested value by the controller.

In this study, the V2G capability, which implies the possibility of reversing the power flow, is not considered and the service provision is possible only by controlling the charging current as defined by IEC 61851 standard [9]. The standard defines that EVs can be controlled by modulating the charging current between 6 and 16 A with 1 A steps. It also defines that EVs have to respond within 3 s and the current has to be limited to the set value. Because of the previous requirements and depending on the EV model and year of production, EVs may show different performances (i.e. the EVs response can vary from under a second to few seconds) [10]. Since this study focuses on synthetic inertia support, the time response is of a crucial importance [11].

In this work, three single-phase EVs are employed to provide synthetic inertia and tested in one islanded configuration of the experimental low-voltage grid SYSLAB PowerLabDK research infrastructure.

2 Methodology

Synthetic inertia in the power system could be emulated if the active power delivered (or absorbed) by the dedicated unit (EVs in this case) is controlled in inverse proportion to the variation of the grid frequency over the time ($\Delta f/\Delta t$) [12]. The experimental set-up and power components are shown in Fig. 1 and detailed in the experimental layout.

2.1 Power components

The experiments are executed in the experimental infrastructure SYSLAB which is part of the PowerLabDK platform.

SYSLAB represents a small-scale low-voltage power system. It consists of a number of real power components interconnected by a three-phase 400 V AC power grid, distributed (>1 km) over the Risø campus of the Technical University of Denmark [7]. SYSLAB is also characterised by its communication and control nodes allowing a strong controllability over the grid and the ability of employing different control architecture (e.g. centralised architecture, distributed architecture). The following components are used during the experiment:

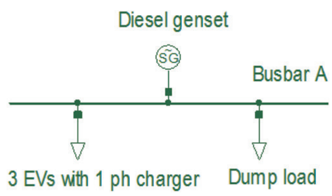

Fig. 1 *Grid layout*

- Three controllable EVs: Two Nissan leaf – each equipped with single-phase 16 A charger and 30 kWh lithium battery storage, both are produced in 2016 (addressed in this work as EV1 and EV3). One Nissan e-NV200 with single-phase 16 A charger and 24 kWh lithium battery storage, produced in 2015 (addressed as EV2).
- Diesel gen-set equipped with a 60 kVA synchronous generator, capable of providing an active power output up to 48 kW.
- A controllable resistive load, named dumpload. The maximum load which is the sum of all the resistors is 78 kW.

All the devices are connected to the same bus-bar and the EVs' initial charging level is chosen, so that there is room to increase and decrease the charging level equally [12].

2.2 EVs controller description

The three single-phase EVs are connected to the grid by means of three electric vehicle supply equipment (EVSE), each connected to a different phase. As the time of response is crucial for the synthetic inertia services and is dependent on the whole control loop, each EV/EVSE pair is controlled independently and in parallel using multithreading.

The communication and control set-up are shown in Fig. 2 and detailed in [10].

It consists of the following components:

- Smart charging controller – receives the measurements from the power meter and sends control signals to the EVSE.
- DEIF MIC-2 – multi-instrument measurement device for voltage, current, and power measurements with 0.5% accuracy. The device is polled every 0.2 s.
- DEIF MTR-3 – multi-instrument measurement device used here for fast frequency measurements.
- EVSE – electric vehicle supply equipment rated for 16 A.
- EV – the three tested EVs.
- Grid – grid connection at the SYSLAB experimental facility.

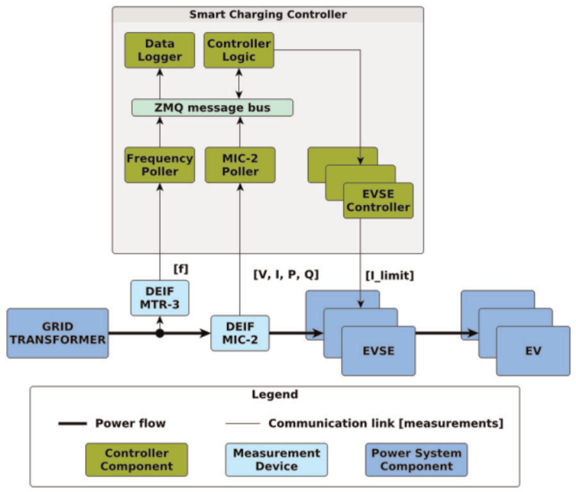

Fig. 2 *Communication and control set-up*

The smart charging controller consists of many subcomponents as described here:

- Controller logic – reads the latest frequency measurements from the message bus and determines the $\Delta f/\Delta t$. It calculates the set-points and sends control signals directly to the EVSE controller.
- EVSE controller – acts as an interface between the physical EVSE and the controller logic.
- Frequency poller – acts as an interface to the frequency measurement devices. In this case, DEIF MTR-3 measurements instrument would be used for frequency sampling every 0.2 s with accuracy of ±10 m Hz.
- MIC-2 poller – multi-instrument interface.
- Data logger – monitors the data exchange on the message bus and logs it to the database.
- ZMQ message bus – message bus used for representing the data exchange between the various components.

3 Experimental set-up and results

The experiments are intended to test the EVs' capability of providing synthetic inertia support limiting the RoCoF in the case of load variations. The experiments are executed in an islanded configuration where the frequency is set by the diesel generator. Three test scenarios are tested, where the frequency variation is triggered by several load events. The load events include an alternate load increase and decrease so that over- and under-frequency dynamics can be investigated. The amplitude of the load event in the three scenarios is equal to 40% of the installed power (i.e. 20 kW), which is 80 times more compared with the expected load step in the European synchronous area. The choice of this large event is to compensate the high inertia value of the diesel gen-set ($2H = 50$ s), allowing for the EVs the time to participate with synthetic inertia support. The diesel's moment of inertia is very high, since it has been designed to operate in island mode.

In this study, the primary frequency control is delivered by the diesel governor and automatically activated by the diesel internal controller, while the secondary frequency control has been disabled.

The three test scenarios are reported below and summarised in Table 1:

(i) 20 kW load power steps from the dumpload to investigate the diesel response and the frequency behaviour. No EVs are connected.
(ii) Load power steps with the EVs controlled by a synthetic inertia controller (controller's thresholds are ±1.5 Hz/s with a deadband (DB) of ±0.8 Hz/s, addressed as α droop).
(iii) Load power steps with the EVs controlled by a synthetic inertia controller (controller's thresholds are ±1 Hz/s with a DB of ±0.35 Hz/s, β droop).

3.1 Scenario 1

In this scenario, only the dumpload and the diesel generator are connected. Since the experiments are performed in island configuration and the diesel governor is active, the scenario aims at investigating if the frequency dynamics are the same for the same load event. For example, investigating if the same load event

Table 1 Components initial conditions and controller parameters

	Components initial conditions			EVs controller parameters	
	Diesel, kW	Load, kW	3 EVs, kW	Thresholds, Hz/s	DB, Hz/s
scen.1	28	28	—	—	—
scen.2	35.5	28	7.5	±1.5	±0.8
scen.3	35.5	28	7.5	±1	±0.35

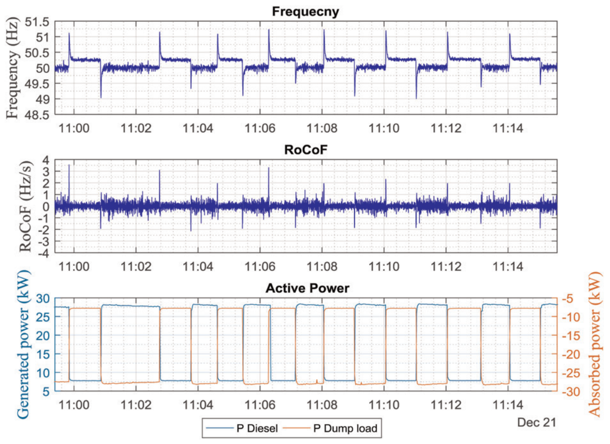

Fig. 3 *Grid frequency, RoCoF, and the absorbed and generated active power*

applied several times implies the same frequency nadir, meaning a precise replicability of the conditions. It is important to note that the RoCoF is determined as $\Delta f/\Delta t$, where the frequency is measured every 0.2 s and therefore Δt is also 0.2 s.

The grid frequency, the RoCoF, and the active power of diesel and dumpload are presented in Fig. 3.

One can notice that, the active power generation and consumption, respectively, from the diesel and the dumpload, are varying with the same amplitude over the time. In theory, this variation should cause the same frequency change over the time.

However, frequency nadir and zenith are not the same over the time. This behaviour is due to the mechanical dynamics of the diesel and small variation in the fuel injection rate during each cycle. Unfortunately, this behaviour limits the possibility of performing a precise comparison of the EVs effects on the RoCoF with and without synthetic inertia support.

In other words, it is not possible to guarantee if the RoCoF improvement is due to the synthetic inertia or to the mechanical dynamics of the diesel. However, it is of high interest to investigate how EVs respond and if the controller and the communication infrastructure are properly designed rather than performing a numerical assessment of the frequency improvement.

3.2 Scenario 2

In this scenario, the diesel generator, the dumpload, and the three EVs are connected. The EVs are equipped with a synthetic inertia controller. The controller calculates the $\Delta f/\Delta t$ and it changes the EVs' current set-point in function of the applied droop. In this study, two different droops are considered: α (the RoCoF limits are ±1.5 Hz/s with a DB of ±0.8 Hz/s) and β (RoCoF limits of ±1 Hz/s and DB of ±0.35 Hz/s). The two droops are RoCoF–current droops and are presented in Fig. 4. The solid lines represent the 1 A step functions implemented in order to comply with the IEC 61851 standard.

The α droop is used in Scenario 2, while the β droop is used in Scenario 3. It is important to highlight that the voltage regulator of

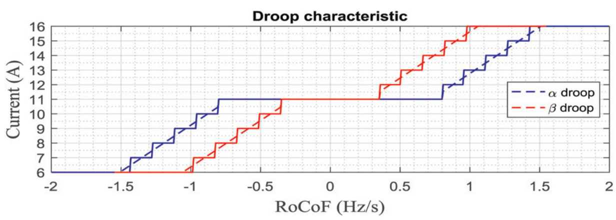

Fig. 4 *Current–RoCoF droop characteristic*

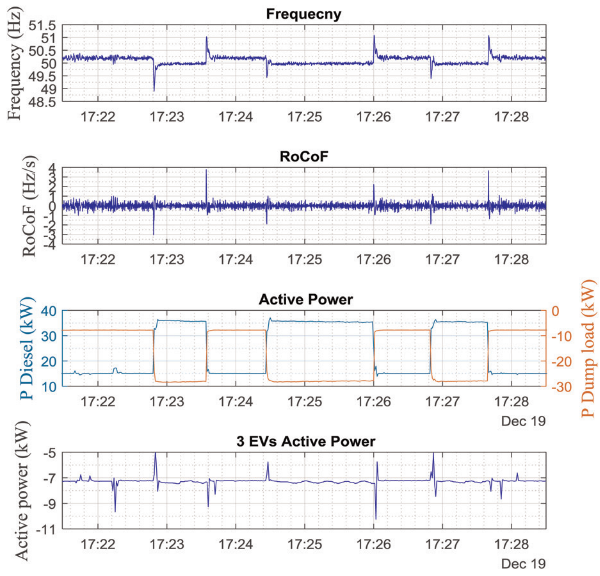

Fig. 5 *Frequency and RoCoF dynamics and the absorbed and generated active power*

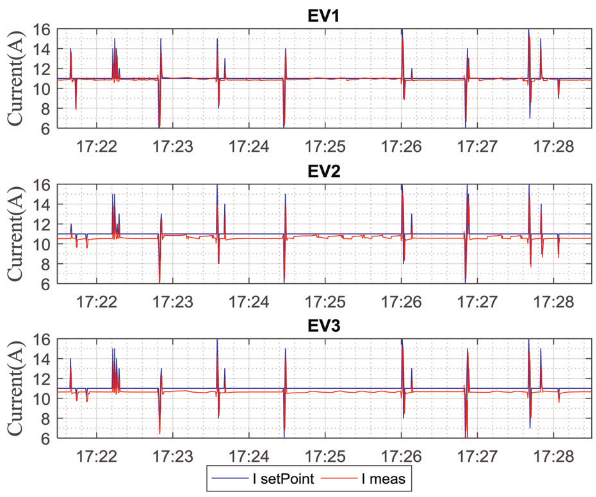

Fig. 6 *EV's current set-point sent by the controller and the EV's measured current*

the diesel tries to maintain the voltage equal to 230 V; therefore, setting the current is like setting the active power.

As for Scenario 1, the load events include an alternate load increase and decrease in the same amplitude, so that over- and under-frequency dynamics can be investigated. The amplitude of the load event is 20 kW.

As it can be seen in Fig. 5, due to the mechanical dynamics, the large inertia value of the diesel, and the limited number of EVs, it is not possible to appreciate improvements in the RoCoF.

However, in Fig. 6, it can be seen that the EVs' current set-point is following the RoCoF variation as desired.

This variation can also be seen in Fig. 7, which shows a zoom of two consecutive load steps. In Fig. 7, only EV1's current is shown. The delay between the current set-point and the absorbed one depends on the EV model and the year of production; in this case, it is in the range of 200–400 ms.

3.3 Scenario 3

This scenario aims at demonstrating the importance of choosing the appropriate controller's thresholds as well as the DB. In this

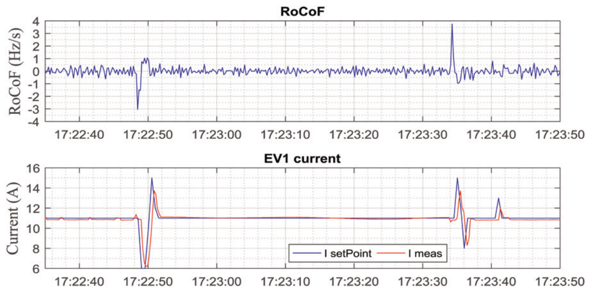

Fig. 7 *RoCoF and EV's current*

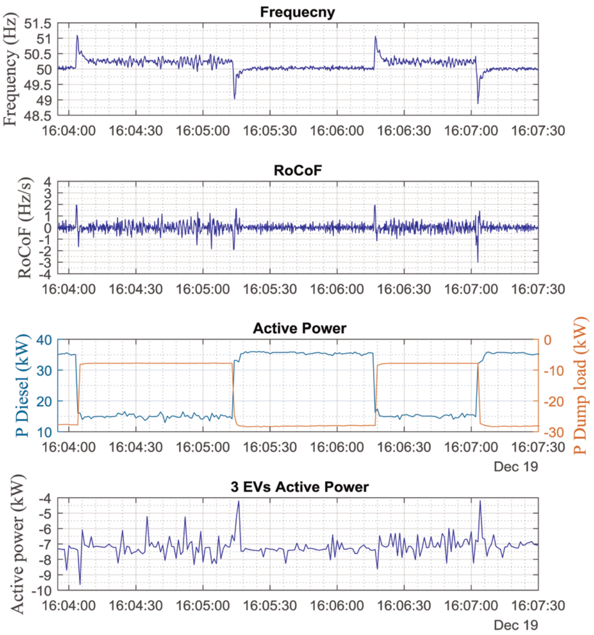

Fig. 8 *Frequency and RoCoF and the absorbed and generated active power*

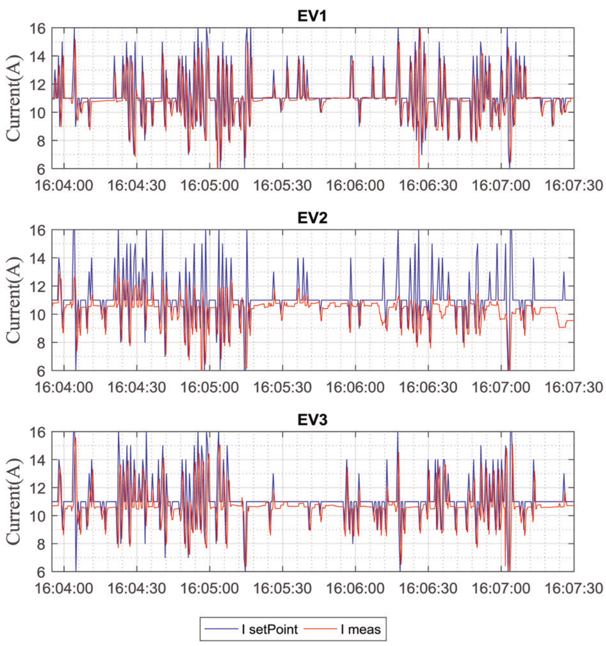

Fig. 9 *EV's current set-point sent by the controller and the EV's measured current*

scenario, the authors decided to apply a higher gain and a smaller DB, namely β droop, to show that on the contrary of the synchronous inertia, synthetic inertia might lead to unstable frequency behaviour if the controller is not well tuned. The results are shown in Figs. 8 and 9, which show the frequency, the RoCoF, and the absorbed and generated power.

On the contrary of the previous scenario, one can notice that the RoCoF is larger which it can be also appreciated from the EVs' current set-point. To prove so, the standard deviation for frequency and RoCoF for Scenarios 2 and 3 is calculated.

For Scenario 2, it is equal to 0.15 Hz and 0.32 Hz/s, respectively, versus 0.19 Hz and 0.39 Hz/s for Scenario 3.

To be mentioned, the grid frequency change and RoCoF are relatively limited due to the diesel large inertia. The smaller DB and the higher gain induce more frequent changes in the current set-point.

One can notice that, due to the different models and production year among the EVs, EV2 founds difficulty in following the set-point as shown in Fig. 9. This difference can be seen as under or overshooting of the measured current as well as a delay between the current set-point and the measured current.

4 Conclusion

The analysis showed the EVs' capability of providing synthetic inertia support. An experimental islanded microgrid has been set, and three series-produced EVs have been controlled relying on synthetic inertia controllers. It was shown that on the contrary of synchronous inertia, more synthetic inertia (achieved by a higher gain and smaller dead band) does not guarantee a slower RoCoF and more stable behaviour. Contrarily, the experiment showed that the higher gain and the smaller DB imposed the EVs to change the current set-point more frequently leading to faster RoCoF. The experiments demonstrated also that even if the EVs are all equipped by the same controller and the same standard (IEC 61851), they do not follow the set-point in the same manner.

Further experiments will be carried out employing a higher number of EVs to appreciate more their effect on the RoCoF in the case of high inertia system as well as low inertia system. Future work will also focus on comparing fast frequency control with synthetic inertia and on the capability of EVs in providing those two services. Namely, employing some EVs for fast frequency control and others for synthetic inertia. Consequently, testing the capability of providing synthetic inertia and fast frequency control from the same unit.

5 Acknowledgments

The work in this paper has been partly supported by the European Commission, under the FP7 project ELECTRA (grant no: 609687) and partly by the Danish research projects Parker (ForskEL kontrakt nr. 2016-1-12410). The authors are also grateful to Nissan Denmark for providing the two Leafs used in the experiments.

6 References

1 Ulbig, A., Borsche, T., Andersson, G.: 'Impact of low rotational inertia on power system stability and operation'. The 19th World Congress of the Int. Federation of Automatic Control, 2014, pp. 1–12
2 The Commission for Energy Regulation: 'Rate of change of frequency (RoCoF) modification to the grid code', 2014
3 Walling, R.A., Miller, N.W.: 'Distributed generation islanding – implications on power system dynamic performance'. Power Engineering Society Summer Meeting, 2002, pp. 92–96
4 EIRGRID and SONI: 'RoCoF alternative & complementary solutions project', 2016
5 Muljadi, E., Gevorgian, V., Singh, M.: 'Understanding inertial and frequency response of wind power plants'. IEEE Symp. on Power Electronics and Machines in Wind Applications, 2012, pp. 1–8

6 Knezovic, K., Martinenas, S., Andersen, P. B., *et al.*: 'Enhancing the role of electric vehicles in the power grid: field validation of multiple ancillary services', *IEEE Trans. Transp. Electrif.*, 2016, **99**, pp. 1–1
7 Marinelli, M., Martinenas, S., Knezovic, K., *et al.*: 'Validating a centralized approach to primary frequency control with series-produced electric vehicles', *J. Energy Storage*, 2016, **7**, pp. 63–73
8 Kempton, W., Tomić, J.: 'Vehicle-to-grid power implementation: from stabilizing the grid to supporting large-scale renewable energy', *J. Power Sources*, 2005, **144**, pp. 280–294
9 IEC 61851-1: 'Electric vehicle conductive charging system – part 1: general requirements', 2010
10 Martinenas, S., Marinelli, M., Andersen, P. B., *et al.*: 'Evaluation of electric vehicle charging controllability for provision of time critical grid services', 2016, pp. 1–5
11 Rezkalla, M., Marinelli, M., Pertl, M., *et al.*: 'Trade-off analysis of virtual inertia and fast primary frequency control during frequency transients in a converter dominated network'. IEEE PES Innovative Smart Grid Technologies – Asia, 2016, pp. 1–6
12 Rezkalla, M., Zecchino, A., Pertl, M., *et al.*: 'Grid frequency support by single-phase electric vehicles employing an innovative virtual inertia controller'. Int. Universities' Power Engineering Conf. – UPEC, 2016, pp. 1–6